

Role of the thermal entrance length on the viscous heating in microchannels

Stéphane Mossaz^{1,2} · Damien Colombet^{1,2} · Gilles Ledoux³ · Frédéric Ayela^{1,2}

Received: 25 March 2015 / Accepted: 8 September 2015 / Published online: 22 September 2015
© Springer-Verlag Berlin Heidelberg 2015

Abstract The present work is devoted to experimental investigations on the viscous heating associated with fluid flows in microchannels with non-adiabatic walls. A very simple model is proposed that demonstrate the relative influence of the thermal entrance length L^* on the temperature rise of a fluid flowing through a rectangular or trapezoidal microchannel. By resolving directly the 1D energy conservation equation, we get an explicit relation describing the evolution of the temperature along the direction of the flow. That model shows that the adiabatic solution is realistic especially when the length of the channel is much lower than L^* . It also demonstrates that when reducing the hydraulic diameter D_h , a steady-state thermal profile is reached and heat losses through the walls considerably limit the temperature rise. Experimental data have been recorded through hybrid silicon–Pyrex trapezoidal microchannels for a large range of hydraulic diameters ($73 \leq D_h \leq 353 \mu\text{m}$) and aspect ratio ($0.05 \leq \chi \leq 0.5$) with isopropanol and ethanol as the working fluids. The experimental data match the values expected from the model that can be useful to predict the order of magnitude of the longitudinal viscous heating in any configuration.

Keywords Microchannels · Viscous heating · Non-adiabatic · Entrance effect

1 Introduction

When a large pressure gradient Δp is applied to a confined fluid to set it in flow, viscous dissipation may lead to an increase in the bulk temperature of the fluid. Such an increase in the temperature results from the conversion of mechanical energy into heat. We consider here a fluid with a negligible thermal coefficient of volume expansion, flowing in a laminar regime through a straight channel, with a density ρ and a specific heat capacity at constant pressure C_p . In perfect adiabatic surroundings laminar flow, the expected temperature rise along the duct ΔT^{adia} obeys the relationship $\Delta P = \rho C_p \Delta T^{adia}$ (Kawashima and Asako 2012). For a fixed pressure drop, the smaller is ρC_p , the more noticeable is thermal rise, which does not depend on the hydraulic diameter D_h of the duct. That effect is usually ignored at macroscale because the turbulent regime is easily reached resulting in an additional axial dispersion that reduces longitudinal heating.

Viscous heating may be crucial for rheological measurements in a narrow slit flow under very high shear rates, because non-isothermal conditions along the flow should affect the values of intrinsic parameters of the fluids such as viscosity. Before the emergence of microtechnologies and microfluidics, Ybarra and Eckert (1980) have performed calculations devoted to determine the local variations of the temperature field in the area where the shear rate reaches a maximum intensity. They have estimated the overall average increase in the fluid's temperature. Their conclusion was that in a parallel plate geometry maintaining walls at a constant temperature, a micro slit rheometer (low D_h) exhibits a global heat exchange coefficient (hS) whose effects are predominant over any bulk effects; using a slit as thin as possible is the solution to minimize unwanted viscous heating.

✉ Damien Colombet
damien.colombet@legi.grenoble-inp.fr

¹ Univ. Grenoble Alpes, LEGI, 38000 Grenoble, France

² CNRS, LEGI, 38000 Grenoble, France

³ Institut Lumière Matière (ILM), UMR5306 Université Lyon 1-CNRS, Université de Lyon, 69622 Villeurbanne Cedex, France

The effects of viscous dissipation in microtubes and microchannels have been scrutinized with a lot of attention in the 2000s, when the validity of the laws of hydrodynamics for microchannels was still not clearly stated. In order to explain some unexpected results relative to the relationship between the pressure drop and the flow rate, some authors have considered the possible influence of the temperature on the Poiseuille number P_o via the strong dependence of the viscosity μ with the temperature (Xu et al. 2003; Koo and Kleinstreuer 2004; Morini 2005; Celata et al. 2006). It was claimed that because of high shear rates, thermal rises were likely to occur in microtubes. Such an assumption is somewhat questionable because it does not take into account the increase in the global thermal exchange coefficient between the fluid and the walls of the microchannel, when D_h is reduced.

So, a fundamental question is to know whether the adiabatic model is still valid to estimate longitudinal heating induced by viscous dissipation in microchannels under ambient conditions. How may the thermal losses be considered as negligible? It is obvious that real microflows will obey an intermediate behaviour between a perfect adiabatic condition and a total heat loss. The heat may be transported in the liquid and/or transferred through the substrate along the axial dimension and perpendicular to the walls (Moharana et al. 2012).

Judy et al. (2002) have reported a maximum rise of 6.2 °C at $Re = 300$ for isopropanol flowing through a fused square microchannel of length $L = 0.114$ m at $D_h = 74.1$ μm . Viscosity based on inlet temperature leads then to an anomalous dependence of P_o with Re , when viscosity based on average temperature leads to the expected constant value P_o . It should be noticed that the operating condition $Re = 300$ corresponds here to a very strong pressure drop $\Delta P \approx 145$ bars and that the recorded temperature rise approaches the expected value given by the adiabatic model. As an example, with water as the working fluid flowing consecutively to a pressure drop of 5 bars, the expected ΔT^{adia} is only around 0.4 °C. Other experimental results have been presented by Celata et al. (2006). The experiments were performed in a vacuum environment to prevent from natural convection at the outer diameter of the tubes. Most of the data display a linear evolution of the temperature rise along the channel with Re that is characteristic of an adiabatic model, although some data at low Re and low D_h deviate from that model.

Nowadays, the controversy about possible deviations of hydrodynamics laws for microchannels is over (Judy et al. 2002; Baviere et al. 2005; Hetsroni et al. 2005). Some authors working with microchannels at $D_h < 50$ μm did not need to adjust the value of the viscosity of the fluid to verify the Poiseuille number. In most of the operating conditions, viscous heating is of a minor importance on the value

of the friction coefficient in microflows. But thermal effects remain of importance for channel capillary microviscometers (Kang and Yang 2013; Morhell and Pastoriza 2013) and for microheat exchangers (Rogiers and Baelmans 2010).

In that problem, fluid velocity and temperature fields cannot develop simultaneously. The hydrodynamical entrance length has to be compared to the thermal entrance length, along which the Nusselt number is not constant (Lee and Garimella 2006; Guidice et al. 2007). It may also be possible that the total length of the channel should be below the hydrodynamical and thermal lengths. The role of the thermal entrance length on the thermal profile and on the Nusselt number Nu should theoretically be considered (Moharana et al. 2012). The role of a thermally developing length has been demonstrated numerically by Koo and Kleinstreuer (2004), who have simulated the evolution of the temperature inside one of the microflows characterized by Judy et al. (2002). Other numerical computations exhibit a quasi-exponential evolution of the temperature along the direction of the flow (Koo and Kleinstreuer 2004; Lelea and Cioabla 2011; Xu et al. 2003). However, these computations cannot offer a versatile equation, able to estimate the order of magnitude of the thermal rise expected from a fixed geometry and under fixed flow conditions.

The objective of the paper is to identify a model able to predict viscous heating in microchannels with non-adiabatic conditions. Experiments have been performed with microchannels for a large range of hydraulic diameter ($73 \leq D_h \leq 353$ μm) and aspect ratio ($0.05 \leq \chi \leq 0.5$). For this purpose, measurements of pressure drop are first taken to confirm a good control of hydrodynamic conditions. Then, accurate measurements of temperature rise along the channels have been taken for isopropanol and ethanol from laminar flow regime up to the turbulent flow regime. The paper is organized as follows. Section 2 describes the experimental set-up. Section 3.1 shows experimental friction factors variations. Section 3.2 presents and discusses the results concerning viscous heating. Section 4 summarizes the main conclusions.

2 Experimental set-up and measurements techniques

Experimental set-up is schematized in Fig. 1a. It is composed of a tank under pressure [1] that contains a membrane filled with liquid. The membrane is pressurized with gaseous nitrogen regulated from a high-pressure bottle [2]. The use of a membrane avoids any gas dissolution into the liquid during the pressurization. A filter [3] is placed after the tank to stop particles larger than 1 μm . The liquid coming from the pressurized tank pass through capillary tubes

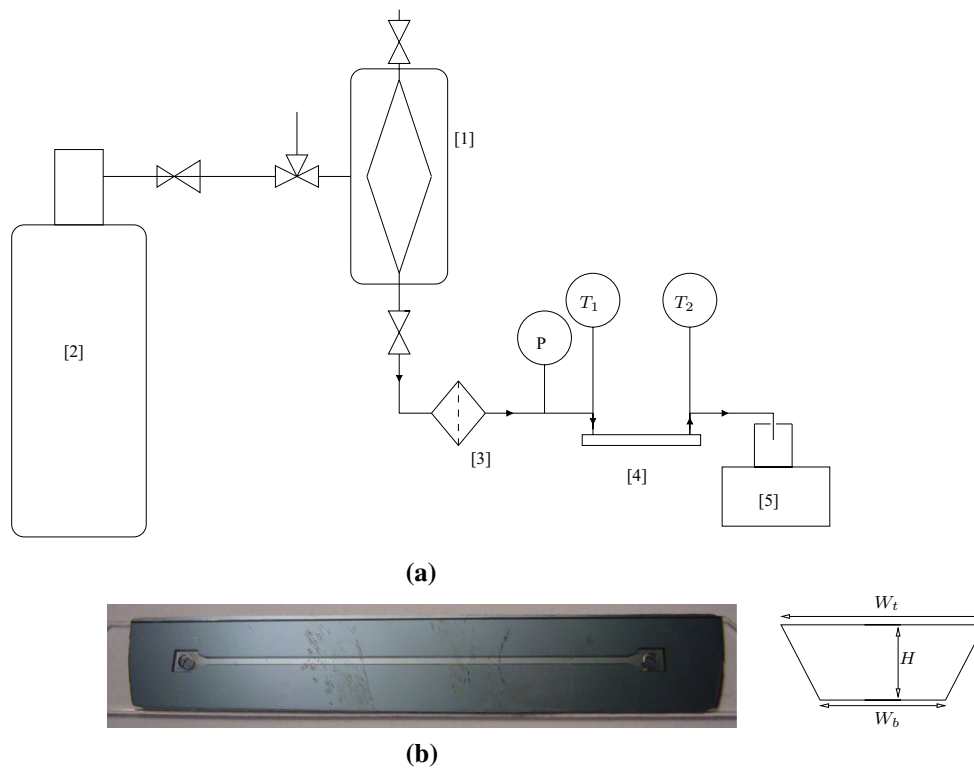


Fig. 1 a Experimental set-up and b silicon–Pyrex microchannel

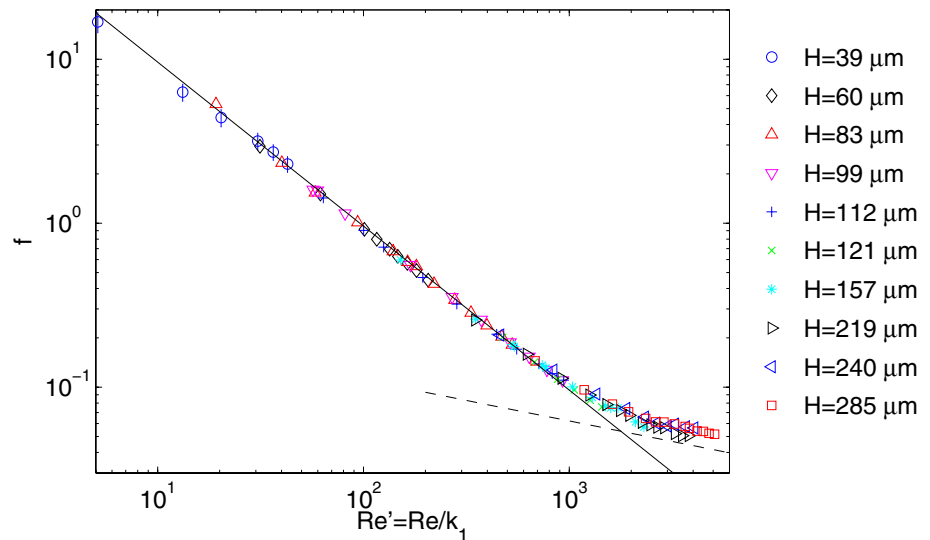
of 2 mm in inner diameter up to the channel that is fixed on 4-mm-thick PVC plate thanks to a stainless steel assembly [4]. The use of a PVC plate under the channel is necessary to insulate the channel bottom from the steel assembly and to ensure that channel walls temperature is mainly controlled by the liquid temperature impacting directly the silicon plate at the inlet. Sealing between the channel and capillary tips is ensured using Viton o-rings that are the only parts in contact with the channel top. The channel sides are only in contact with the air. Thanks to a precision balance [5] (Kern GS410-3), the mass flow rate is deduced by measuring the amount of liquid flowed through the channel for a given duration. The uncertainty on the measurement of the amount of liquid is set to correspond to one drop of liquid ± 50 mg. The uncertainty on the time of measurement is estimated to be around ± 0.5 s. A photograph of one of the channels under investigation is displayed in Fig. 1b. The channels are first etched in a silicon wafer of thickness $e = 320 \mu\text{m}$ ($8 \text{ mm} \times 5 \text{ cm}$) in a chemical KOH solution providing smooth walls. A Pyrex plate of thickness $e = 300 \mu\text{m}$ pierced at its extremities is then anodically bonded onto the silicon channel. Channels studied in this work are characterized by a trapezoidal cross section with a geometric apex angle around $\psi = 54.7^\circ$. Channel's height H , top W_t and bottom W_b widths are given in Table 1 with hydraulic diameter D_h and aspect ratio defined as

$\chi = H / [(W_b + W_t) / 2]$. The channel dimensions have been accurately measured using a stylus profiler (Veeco dektak 6M). The uncertainty on measurements of W_b and W_t is estimated to be $\pm 1 \mu\text{m}$. The corresponding uncertainty associated with the hydraulic diameter D_h is estimated to be around $\pm 3 \mu\text{m}$. The channel length is fixed to $L = 4 \text{ cm}$ for all experiments. The channel width is around $770 \mu\text{m}$, and the channel height varies between 39 and $285 \mu\text{m}$ so that the hydraulic diameter lies between 73 and $353 \mu\text{m}$. The relative pressure is measured after the filter [3], just before the channel inlet using a highly precise pressure transmitter (Keller, PR33X) that ensures an uncertainty of $\pm 2000 \text{ Pa}$. The friction factor corresponding to regular (or linear) pressure drop is measured from Darcy equation

$$f = \frac{D_h}{L} \frac{\Delta p}{(1/2)\rho U^2} \tag{1}$$

where Δp is the pressure difference between channel inlet and outlet and $D_h = 4 A/P$ is the hydraulic diameter based on channel trapezoidal cross section A and perimeter P . $U = Q_v/A = Q_m/(\rho A)$ is the surface average velocity. Two thermo-resistive microprobes (A Class PT100) of 0.5 mm in diameter are installed at the inlet and outlet of the channel thanks to T connexions. To measure accurately the platinum resistance variation, the temperature measurement is taken with a 4-wire connection. The probes are calibrated

Fig. 2 Friction factor f (Eq. 1) versus modified Reynolds number Re' for experiments with isopropanol; Exp. data: symbols; *line* indicates theory for laminar flow f_{lam} ; *dotted line* indicate theory for turbulent flow f_{turb}



to ensure an uncertainty of ± 0.025 K. During the experiments, a monitoring of temperature measurement shows that a steady-state viscous heating is reached for a duration varying between 3 min for high flow rates until to 20 min for low flow rates. Density ρ , dynamic viscosity μ , thermal conductivity λ and heat capacity C_p are estimated using literature correlations. Since measured longitudinal temperature increases are lower than $\Delta T = 1$ °C, fluid properties are considered to be constant and are calculated using the average temperature of the fluid in the channel ($T = [T_1 + T_2]/2$). Table 2 presents fluid properties for $T = 20$ °C. The uncertainties associated with density and viscosity are, respectively, estimated as ± 10 kg m $^{-3}$ and ± 0.0002 Pas. The corresponding uncertainty on Reynolds number is about ± 10 % for high Re and ± 20 % for low Re .

3 Results and discussion

In the first section, experimental results on pressure drops in microchannels are presented in terms of friction factor and compared to correlations available in the literature for the case of a rectangular channel. In the second section, experimental results on viscous heating along the channel are presented and compared to a theoretical one in non-adiabatic conditions. In Fig. 2, error bars indicate the uncertainty related to channel size, to liquid density, and to the measurements of pressure drop and mass flow rate. In this figure, only error bars larger than symbols are displayed. In Figs. 3 and 4, only experimental results with measured viscous heating larger than 0.09 °C are considered and error bars indicate uncertainty related to temperature measurements.

Table 1 Trapezoidal microchannels dimensions and dimensionless numbers for isopropanol experiments

No.	H (μm)	W_b (μm)	W_t (μm)	D_h (μm)	χ (%)	β (%)	Re	G_z	$Nu(\chi)$	L/L^*	$Nu(\chi, G_z)$	L/L^*
1	39	696	760	73	5.4	5.6	5–42	2.5–3.5	6.28	7.1–9.9	–	–
2	49	678	755	92	6.8	7.2	–	–	–	–	–	–
3	60	678	767	108	8.3	8.8	90–185	12–21	5.80	1.0–1.9	–	–
4	83	641	762	145	11.8	12.9	81–456	18–70	5.26	0.3–1.12	6.5–8.0	0.5–1.4
5	99	639	779	169	14.0	15.5	143–783	25–134	4.97	0.15–0.78	6.5–9.1	0.27–1.02
6	112	598	760	186	16.5	18.7	103–772	50–164	4.66	0.11–0.36	7.0–9.4	0.22–0.55
7	121	589	763	198	17.9	20.5	385–1169	78–232	4.49	0.07–0.23	7.5–10.4	0.17–0.38
8	157	543	772	243	23.9	28.9	405–1767	107–452	3.89	0.03–0.15	7.7–12.6	0.11–0.28
9	219	450	763	304	36.2	48.7	640–2657	280–841	3.10	0.01–0.04	9.9–16.2	0.07–0.14
10	240	439	777	324	39.5	54.7	926–2773	316–937	2.97	0.01–0.03	10.2–15.7	0.07–0.13
11	285	367	772	353	50.0	77.7	1050–3294	405–1218	2.68	0.01–0.03	11.0–16.9	0.06–0.10

Fig. 3 (Colour online) Viscous heating versus Reynolds number Re with isopropanol; Exp. data: symbols; *line* indicates theory with heat loss at channel wall (Eq. 5) where Nusselt is estimated from Eq. 6 valid for fully developed temperature profile; *dotted line* indicates theory with heat loss (Eq. 5) where Nusselt is estimated from Eq. 8 valid for developing temperature profile

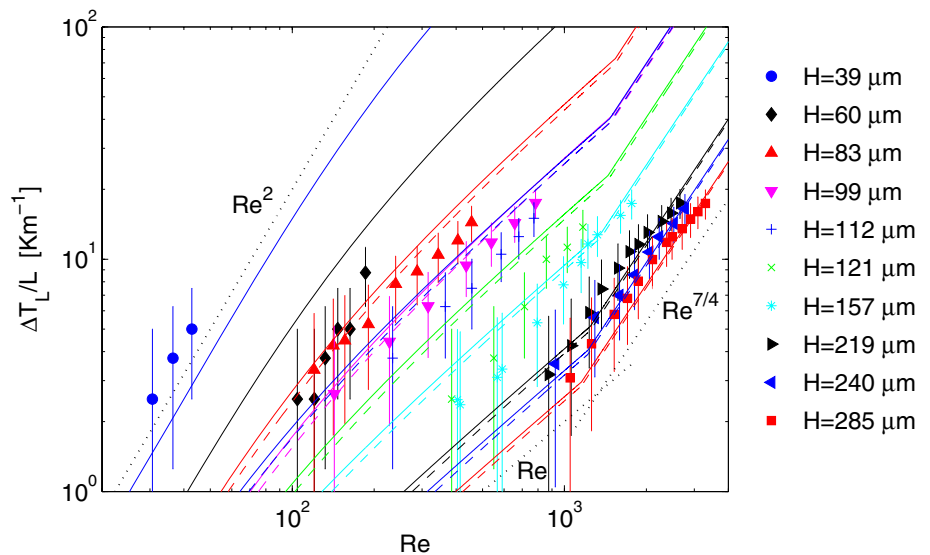
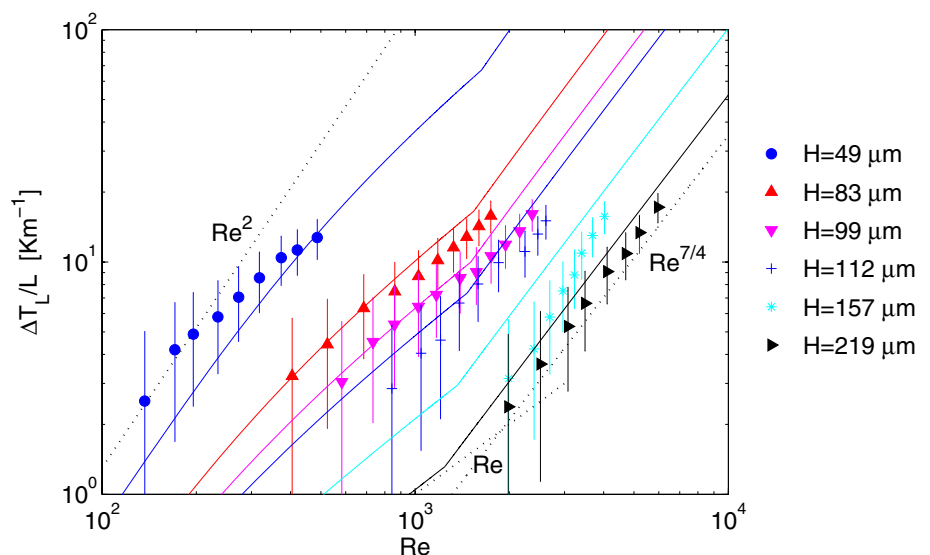


Fig. 4 (Colour online) Viscous heating versus Reynolds number Re with ethanol; Exp. data: symbols; theory with heat loss (Eq. 5) where Nusselt is estimated from Eq. 6



3.1 Friction factor

First, it has been checked that the length required to reach a fully developed velocity profile L_H is much smaller than the channel length L for all experiments presented in this work ($L_H/L < 10\%$). The variation of the friction factor (Eq. 1) is presented in Fig. 2 versus the modified Reynolds number $Re' = Re/k_1$ introduced by Jones (1976) where $Re = \rho U D_h / \mu$ and k_1 is calculated here using the relation proposed by Guyer (1989)

$$k_1 = 1 - 1.3553\chi + 1.9467\chi^2 - 1.7012\chi^3 + 0.9564\chi^4 - 0.2537\chi^5 \quad (2)$$

The introduction of the Reynolds number Re' enables here to take into account the effect of the aspect ratio variation χ on the friction factor f . As expected, in laminar flow region, the friction factor decreases with Reynolds number

up to the transition regime to turbulent flow. As reported in Fig. 2, experimental measurements are found to be in good agreement with the theory for laminar flow $f_{lam} = 96/Re'$ and for turbulent flow $f_{turb} = 0.3164/(Re'/1.5)^{1/4}$ in rectangular cross-sectional channel (see Jones (1976) and Idel'cik (1986)). Note that Poiseuille number in laminar flow is as expected $P_o = fRe'/4 = 24$. For laminar flow experiments, average relative difference between measurements and theory is only of 7 %. Note that this result is consistent with several previous works (Judy et al. 2002; Baviere et al. 2005; Hetsroni et al. 2005) that have shown that regular pressure drop correlations conventionally used for macrosized channels are still valid for microchannels. The very good matching between friction factor predictions and measurements indicates therefore that experiments are performed in validated hydrodynamic conditions with a fully developed velocity profile. As expected, the end of

Table 2 Fluid properties for $T = 20\text{ }^\circ\text{C}$ from Yaws (1999) and ^aBrown and Ziegler (1979)

	ρ (kg m ⁻³)	μ ($\times 10^{-3}$ Pa s)	C_p (J kg ⁻¹ K ⁻¹)	λ (W m ⁻¹ K ⁻¹)	Pr
Isopropanol	787.5	2.288	2511 ^a	0.14	47.0
Ethanol	791.9	1.162	2319	0.17	15.7

laminar regime and the beginning of turbulent regime are found to correspond roughly to $Re \approx 1000 - 2000$ and $Re' \approx 1300$.

3.2 Viscous heating along the channel

Considering a steady-state fully developed flow, viscous heating along the channel can be described solving energy conservation equation in one dimension as follows

$$\underbrace{\rho C_p U \frac{\partial T}{\partial x}}_{A-\text{axial-convection}} = \underbrace{(\lambda + \lambda^T) \frac{\partial^2 T}{\partial x^2}}_{B-\text{axial diffusion}} + \underbrace{-U \frac{\partial P}{\partial x}}_{C-\text{viscous heating}} - \underbrace{S\phi}_{D-\text{heat losses}} \quad (3)$$

The A term stands for the axial convection transport of energy. B is the sum of the laminar (λ) and turbulent (λ^T) axial energy transport by diffusion. λ^T corresponds here to turbulent conductivity induced by turbulent axial flux. C is the source term induced by viscous heating, and D is the sink term due to heat losses through channel walls. ϕ is heat flux per surface unit due to heat losses at channel wall. $S = S_{lat}/V_{liq} = 4/D_h$ is the heat exchange surface per liquid volume unit corresponding to lateral channel walls. In Eq. 3, each variable is surface averaged on the channel cross section and the x-axis is the channel axis. For laminar flow, which is usually found in microfluidics, the turbulent transport does not occur and $\lambda^T = 0$. In addition, using dimensional analysis, one can easily show that axial transport of heat by diffusion (B term with λ) can be neglected compared to other terms for large axial Peclet number $Pe_L = UL/\alpha \gg 100$ where $\alpha = \lambda/(\rho C_p)$ is the thermal diffusivity. Peclet number based on channel length compared characteristic time of heat transport by diffusion (L^2/α) to characteristic time of heat transport by convection (L/U) along the channel. In the present experiments with isopropanol, the Prandtl number stays around $Pr = \mu/(\rho\alpha) \approx 45$ and thermal Peclet number variation range is $8 \times 10^5 < Pe_L < 157 \times 10^5$ so that term B (axial heat diffusion) in Eq. 3 can be neglected. For experiments with ethanol, term B can also be neglected in Eq. 3 since we have $Pr \approx 15$ and $2 \times 10^5 < Pe_L < 120 \times 10^5$.

For the case of adiabatic walls, only terms A and C are predominant and the solution of Eq. 3 is simply $\Delta T^{adia} = \Delta P/(\rho C_p)$ (Morini 2005; Kawashima and Asako 2012). This model is found to be in good agreement with

experiments of Celata et al. (2006) where microchannels are placed in a chamber under vacuum. In the absence of heat flux at channel walls, the evolution of f with Re (Fig. 2) implies that viscous heating should be proportional to $\Delta T \propto Re$ for laminar flow and to $\Delta T \propto Re^{7/4}$ for turbulent flow, for a given liquid and channel geometry. However, $\Delta T = \Delta T^{adia}$ is only valid for channels with adiabatic walls, and we are aiming in this work to take into account heat losses through channel walls. We assume here that heat loss flux can be described by heat transfer with imposed temperature T_w at the channel walls so that $\phi = h(T - T_w)$ where $h = Nu \lambda/D_h$ is heat transfer coefficient based on Nusselt number Nu . In addition, because of the presence of a PVC-insulated plate under each channel, we assume that channel wall temperature is imposed by liquid inlet temperature so that the conduction in Pyrex and silicon set the channel walls temperature to $T_w = T_1$. As a result, Eq. 3 with $B=0$ can be written as follows

$$\rho C_p U \frac{\partial T(x)}{\partial x} = -U \frac{\partial P}{\partial x} - Sh(T(x) - T_1) \quad (4)$$

with $\partial P/\partial x = -\Delta T^{adia} \rho C_p/L < 0$ the pressure gradient that is constant along the channels. Eq. 4 traduces the balance between the viscous heating in the liquid bulk, which does not depend on T, and the heat losses through the walls, which depends on $T(x)$. The solution of this first-order differential equation is then with $\Delta T(x) = T(x) - T_1$

$$\Delta T(x) = \Delta T^{adia} \frac{L^*}{L} \left[1 - \exp\left(\frac{-x}{L^*}\right) \right] \quad \text{with } L^* = \frac{Re Pr D_h}{4Nu} \quad (5)$$

where L^* is a characteristic length related to the development of heat transfer at walls along the channel. Equation 5 exhibits the difference between the thermally fully developed flow and the thermally developing flow. The thermally developed flow condition $L \gg L^*$ is usually satisfied for smallest Re values and/or for smallest hydraulic diameters D_h . With such a condition, the longitudinal thermal rise is $\Delta T_L = \Delta T(x=L) = \Delta T^{adia} L^*/L \ll \Delta T^{adia}$. This is because surface effects are predominant over bulk effects in microfluidics; the smaller the D_h is, the higher the surface exchange coefficient $h \times S$ is. That is consistent with the theoretical average temperature variations reported by Ybarra and Eckert (1980) for longitudinal viscous heating with a constant wall temperature. Considering the evolution of ΔT^{adia} and L/L^* with Re , an evolution of ΔT_L proportional to Re^2 and $Re^{11/4}$ is then expected for, respectively, laminar and turbulent flow when $L \gg L^*$. Since the average Nusselt

number Nu for imposed wall temperature depends closely on channel aspect ratio and shape, the relation proposed by Renksizbulut and Niazmand (2006) for fully developed heat transfer in trapezoidal channels can be applied, for $0.1 \leq Re \leq 1000$

$$Nu(\chi) = \left[2.87 \left(\frac{90}{\psi} \right)^{-0.26} + 4.8 \exp \left(-3.9\beta \left(\frac{90}{\psi} \right)^{0.21} \right) \right] k_2$$

with $k_2 = 1 + 0.075(1 + \beta) \exp(-0.45Re)$ (6)

with the apex angle $\psi = 54.7$ in degree and the aspect ratio based on the bottom width $\beta = H/W_b$. The correction factor k_2 takes into account axial conduction effects on heat transfer for the case $Pe_L \ll 1$. For present experiments where $\beta < 1$ and $Re > 10$, we have $k_2 = 1$ and Nusselt number depends only on channel geometry (ψ and β). This relation predicts a Nusselt number a little lower than the one corresponding to a rectangular cross-sectional channel of same aspect ratio χ . For example, for isopropanol, with channel N°1 (N°11) Nusselt number with Eq. 6 is 4 % (20 %) lower than the one given for a rectangular channel (Shah and London 1971). For a fully developed temperature field, it is possible, from Eq. 6, to calculate Nusselt number and thus L/L^* for laminar microflows and wall-imposed temperature (see Table 1). The determination of the heat transfer coefficient h is performed from the Nusselt number. The corresponding values confirm that the choice of an imposed temperature as wall boundary condition is relevant since corresponding Biot number for the silicon substrate $Bi = h(V_{\text{silicon}}/S_{\text{lat-silicon}})/\lambda_{\text{silicon}} \approx 0.02 - 0.3$ is very low so that strong temperature gradients inside it are unlikely. In addition, Biot number of the Pyrex cover plate is $Bi = h(V_{\text{pyrex}}/S_{\text{lat-pyrex}})/\lambda_{\text{pyrex}} \approx 40 - 50$ so that temperature gradient inside it stays moderate.

The condition $L \ll L^*$, corresponding to a thermally developing flow, is likely to occur for large values of the product $RePrD_h$. A second-order Taylor series expansion of Eq. 5 for $L/L^* \rightarrow 0$ gives

$$\Delta T_L(L \ll L^*) \approx \Delta T^{adia} (1 - 2Nu/G_z) \tag{7}$$

with the Graetz number defined as $G_z = RePr/(L/D_h) = 4NuL^*/L$. Thermally developed flows correspond to small G_z numbers. For thermally developing flows (large G_z), Nusselt number varies along the channel and its mean value increases with G_z (Brown 1960; Wibulswas 1966). In the literature, to our knowledge, no relation has been identified to predict entrance effect on Nusselt number for trapezoidal cross-sectional microchannels with a constant wall temperature. However, direct numerical simulations of wall-imposed temperature heat transfer in rectangular cross-sectional microchannel have been performed by Lee and Garimella (2006). Authors found that average Nusselt number for entrance region

(Eq. 13 in the paper) is well described using the following correlations for $0.1 \leq \chi \leq 1$ and $G_z > 55$

$$Nu(\chi, G_z) = Nu(\chi) + (k_3 G_z^{-0.64} + k_4)^{-1}$$

with $k_3 = -2.757 \times 10^{-3} \chi^{-3} + 3.274 \times 10^{-2} \chi^{-2}$
 $- 7.464 \times 10^{-5} \chi^{-1} + 4.476$ (8)
 $k_4 = 1.604 \times 10^{-4} \chi^{-2} - 2.622 \times 10^{-3} \chi^{-1}$
 $+ 2.568 \times 10^{-2}$

According to this relation, in agreement with previous works, $Nu(\chi, G_z)$ approaches $Nu(\chi)$ for moderate G_z . For large Graetz number, Eq. 8 tends to a maximal finite value of $Nu(\chi, G_z \rightarrow \infty) = Nu(\chi) + k_4^{-1} \approx 70$. As shown by Eq. 7, large G_z numbers demonstrate that quasi-adiabatic conditions reign as long as the thermal field and thus heat transfer are not fully developed. Therefore, for low values of L/L^* or low ratio Nu/G_z , similarly to adiabatic conditions, an evolution of ΔT_L proportional to Re (laminar flow) or $Re^{7/4}$ (turbulent flow) is then expected.

In Table 1 are summarized the dimensionless numbers $Re, Nu, L/L^*$ and G_z , calculated with isopropanol as the working fluid under test. The ratio L/L^* has been first calculated by using Eq. 6. The dependance of Nu with G_z has then been taken into account for the channels exhibiting a ratio $L/L^* < 1$.

The experimental data are reported in Fig. 3, where $\Delta T_L/L$ is plotted as a function of Re . The data are compared to the predicted temperature rises provided by Eq. 5 with $Nu = Nu(\chi)$ (solid lines) and $Nu = Nu(\chi, G_z)$ (dashed lines), where ΔT^{adia} is estimated from the theoretical pressure loss ($f_{\text{lam}}, f_{\text{turb}}$). The results recorded with $H = 39$ and $60 \mu\text{m}$ demonstrate for both channels that ΔT_L increases as Re^2 . Such an evolution agrees with Eq. 5. The fact that ΔT_L remains below ΔT^{adia} confirms that a thermally developed flow is reached and that viscous heating is minimized by the enhancement of heat losses. The results recorded with the three channels obeying $H \geq 219 \mu\text{m}$ demonstrate that ΔT_L increases as $Re^{7/4}$. That agrees with the extrapolation provided by Eq. 7 corresponding to turbulent regime and poorly developed temperature profile ($L/L^* \ll 1$). Other experimental data corresponding to $100 < Re < 1000$ are also consistent with Eq. 5. In addition, taking into account the effect of G_z on Nusselt number improves predicted thermal rises for channels with heights $60 \mu\text{m} \leq H \leq 219 \mu\text{m}$. For larger D_h corresponding to low L/L^* , the dependence of Nu to G_z becomes negligible since when increasing G_z Nusselt number variations are minimized (Eq. 7). This behaviour is also due to the increase in D_h that induces a strong decrease in heat transfer coefficient $hS = 4Nu \lambda/D_h^2 \propto D_h^{-2}$ so that in Eq. 3 term D due to heat losses becomes negligible compared to term A and C ($B = 0$). As a consequence, since Nusselt

variation induced by Graetz number increase has a marginal effect, at first order, it can be concluded that the main parameters to estimate the viscous heating are the theoretical temperature rise in adiabatic conditions ΔT^{adia} and the length ratio $L/L^* = 4Nu/Gz$.

To confirm the validity of this model, experiments with ethanol have been also conducted for $92 \leq D_h \leq 304 \mu\text{m}$ and $136 \leq Re \leq 5960$. As for isopropanol (Fig. 2), it is found that friction factor obtained with ethanol obeys the theory. Thermal rises obtained with ethanol are compared to Eq. 5 with $Nu(\chi)$ in Fig. 4. As shown in this figure, the same scale laws are found and the agreement with experiments is good. In addition, for practical applications, it is interesting to note that for channels with small height ($Nu = 7.54, f = 96/Re$) verifying $L/L^* > 4$ (i.e. $Nu/Gz > 1$) under laminar flow, viscous heating should be simply $\Delta T = 1.6PrU^2/C_p$. The validity of that last expression may be checked with the experimental data: a temperature rise of $\Delta T = 0.1 \text{ }^\circ\text{C}$ for isopropanol flowing through the channel $N^\circ 1 (H = 39 \mu\text{m})$ should correspond to $Re \approx 40$, and for ethanol flowing through the channel $N^\circ 2 (H = 49 \mu\text{m})$, it should correspond to $Re \approx 190$. Those values are globally in agreement with experimental observations. Remaining discrepancies between measured viscous heating and Eq 5 may be due to a coupling between viscous heating in the fluid and heat transfer by conduction inside the silicon–Pyrex blocks ($T_w \neq T_1$, Qu and Mudawar 2002; Kosar 2010). Nevertheless, the model presented here explains the discrepancy with adiabatic theory and is able to give the order of magnitude of viscous heating with heat losses.

Relation 5 is now compared to the numerical simulations performed by Koo and Kleinstreuer (2004) (see Fig. 3 in ref.). We consider a $D_h = 74.1 \mu\text{m}$ square channel ($Nu = 3$) where $L/D = 1543$, with $Re = 300$. These conditions correspond to $\Delta T^{adia} = 0.6, 6$ and $1 \text{ }^\circ\text{C}$ for water, isopropanol and methanol as the working fluids respectively. For the same fluids, the thermal entrance length ratio are, respectively, $L^* = 11, 69$ and 19 mm . The analytical results from Eq. 5 are, respectively, $\Delta T_L = 0.6, 4.8$ and $1 \text{ }^\circ\text{C}$. The evolution $\Delta T(x)$ and the longitudinal temperature rise ΔT_L are found to be in a good agreement with their computational curves and with longitudinal viscous heating measured by Judy et al. (2002) for isopropanol ($\Delta T_L = 6.2 \text{ }^\circ\text{C}$). The numerical calculations, based on the whole terms of the energy conservation (Eq. 3), are the only way to reach the exact thermal profile of the flow. However, our simple model, which enhances the physical role of the thermal entrance length, gives a comprehensive determination of the possible temperature rises of the microflow.

A final question of interest is the effect of turbulence on viscous heating. The presence of turbulence may first

increase axial mixing resulting in lower inlet/outlet temperature rise ($\lambda^T \neq 0$ in Eq. 3). Secondly, the development of mean temperature profile and heat flux at channel walls should also be modified by local turbulent transport so that Nusselt number may also be enhanced at the entrance region (Al-Arabi 1982; Nancy et al. 2014). For $L/L^* < 0.20$, it is found that measured temperature rises seem to reach a plateau corresponding to $\Delta T_L/\Delta T^{adia} \approx 0.7 - 0.8$ for $Re > 3000$. Such a behaviour may be the result of the enhancement of heat axial transport induced by the turbulence. In the present work, for thermally developing flows (low L/L^*), a reasonably good estimation of viscous heating is still given by Eq. 5 up to a Reynolds number of 5960.

4 Conclusion

Viscous heating in straight microchannels at ambient temperature has been investigated for the case of non-adiabatic walls in well-controlled hydrodynamic conditions. The proposed model shows that the thermal length L^* related to temperature profile development with heat losses along the channel appears to be very important for the prediction of viscous heating in microchannels. In addition, for present experiments, this parameter is found to be preponderant compared to average Nusselt number increase due to heat transfer development along the channel. In the limit of $L/L^* = 4Nu/Gz \rightarrow 0$, the decrease in heat losses compared to viscous heating makes the model to tend to a temperature rise approaching the one expected in adiabatic conditions so that $\Delta T_L \approx \Delta T^{adia}$. For such length ratio, scale laws expected are $\Delta T_L \propto Re$ for laminar flow and $\Delta T_L \propto Re^{7/4}$ for turbulent flow. In the limit of $Nu/Gz > 1$, the present model shows that viscous heating results from an equilibrium between heat production in liquid bulk and heat losses through channel walls and tends to $\Delta T_L \approx \Delta T^{adia} Gz/(4Nu) < \Delta T^{adia}$. For such ratio, the increase in temperature along the channel is expected to be proportional to $\Delta T_L \propto Re^2$ for laminar flow and $\Delta T_L \propto Re^{11/4}$ for turbulent flow. The scale laws of $\Delta T_L (Nu/Gz > 1) \propto Re^2$ in laminar regime and $\Delta T_L (Nu/Gz \rightarrow 0) \propto Re^{7/4}$ in turbulent regime seem to be confirmed by present experimental results with isopropanol and ethanol. For intermediate value of Nu/Gz , the complete model has to be considered (Eq. 5). This model still gives a realistic approximation of viscous heating in microchannels for Reynolds number up to $Re = 6000$ and thermally developing flows. Further investigations are needed to identify the effect of turbulence on viscous heating in microchannels for large Reynolds number and thermally fully developed flows.

Acknowledgments This work has been partially supported by the LabEx Tec 21 (Investissements d’Avenir-Grant agreement No ANR-11-LABX-0030). The authors acknowledge helpful assistance of the technical support of the staff of the Nanofab facilities from the Néel Institute of Grenoble. We also thank Jean-Marc Barnoud from LEGI for his help in the fabrication of the experimental set-up.

References

- Al-Arabi M (1982) Turbulent heat transfer in the entrance region of a tube. *Heat Transf Eng* 3:76–83
- Baviere R, Ayela F, Le Person S, Favre-Marinet M (2005) Experimental characterization of water flow through smooth rectangular microchannels. *Phys Fluids* 17:098105
- Brown G (1960) Heat or mass transfer in a fluid in laminar flow in a circular or flat conduit. *AIChE J* 6:179–83
- Brown G, Ziegler W (1979) Temperature dependence of excess thermodynamic properties of ethanol + n-heptane and 2-propanol + n-heptane solutions. *J Chem Eng Data* 24:319–330
- Celata P, Morini G, Marconi V, McPhail S, Zummo G (2006) Using viscous heating to determine the friction factor in microchannels—an experimental validation. *Exp Therm Fluid Sci* 30:725–731
- Del Giudice S, Nonino C, Savino S (2007) Effects of viscous dissipation and temperature dependent viscosity in thermally and simultaneously developing laminar flows in microchannels. *Int J Heat Fluid Flow* 28:15–27
- Guyer E (1989) *Handbook of applied thermal design*. McGraw-Hill, New York
- Hetsroni G, Mosyak A, Pogrebnayk E, Yarin L (2005) Fluid flow in micro-channels. *Int J Heat Mass Transf* 48:1982–1998
- Idel’cik I (1986) *Mémento des pertes de charges*. Eyrolles, Paris
- Jones O (1976) An improvement in the calculation of turbulent friction in rectangular ducts. *J Fluid Eng* 98:173–180
- Judy J, Maynes D, Webb B (2002) Characterization of frictional pressure drop for liquid flows through micro-channels. *Int J Heat Mass Transf* 45:3477–3489
- Kang Y, Yang S (2013) Integrated microfluidic viscometer equipped with fluid temperature controller for measurement of viscosity in complex fluids. *Microfluid Nanofluid* 14:657–668
- Kawashima D, Asako Y (2012) First law analysis for viscous dissipation in liquid flow in micro-channels. *Int J Heat Mass Transf* 55:2244–2248
- Koo J, Kleinstreuer C (2004) Viscous dissipation effects in microtubes and microchannels. *Int J Heat Mass Transf* 47:3159–3169
- Kosar A (2010) Effect of substrate thickness and material on heat transfer in microchannel heat sinks. *Int J Heat Mass Transf* 49:635–642
- Lee P, Garimella S (2006) Thermally developing flow and heat transfer in rectangular microchannels of different aspect ratios. *Int J Heat Mass Transf* 49:3060–3067
- Lelea D, Cioabla A (2011) The developing heat transfer and fluid flow in micro-channel heat sink with viscous heating effect. *Heat Mass Transf* 47:751–758
- Moharana M, Singh P, Khandekar S (2012) Optimum nusselt number for simultaneously developing internal flow under conjugate conditions in a square microchannel. *J Heat Transf* 134:071703
- Morhell N, Pastoriza H (2013) A single channel capillary microviscometer. *Microfluid Nanofluid* 15:475–479
- Morini G (2005) Viscous heating in liquid flows in micro-channels. *Int J Heat Mass Transf* 48:3637–3647
- Narcy M, de Malmazet E, Colin C (2014) Flow boiling in tube under normal gravity and microgravity conditions. *Int J Multiph Flow* 60:50–63
- Qu W, Mudawar I (2002) Analysis of three-dimensional heat transfer in micro-channel heat sinks. *Int J Heat Mass Transf* 45:3973–3985
- Renksizbulut M, Niazmand H (2006) Laminar flow and heat transfer in the entrance region of trapezoidal channels with constant wall temperature. *J Heat Transf* 128:63–74
- Rogiers F, Baelmans M (2010) Towards maximal heat transfer rate densities for small-scale high effectiveness parallel-plate heat exchangers. *Int J Heat Mass Transf* 53:605–614
- Shah R, London A (1971) Laminar flow forced convection heat transfer and flow friction in straight and curved ducts. Technical Report N 75, Dpt Mech Ing, Stanford University
- Wibulswas P (1966) Laminar flow heat transfer in non circular ducts. PhD thesis, London University
- Xu B, Ooi K, Mavriplis C, Zagloul ME (2003) Evaluation of viscous dissipation in liquid flow in microchannels. *J Micromech Microeng* 13:53–57
- Yaws C (1999) *Chemical properties handbook: physical thermodynamic environmental transport safety and health related properties for organic and inorganic chemicals*. McGraw-Hill Education, New York
- Ybarra R, Eckert R (1980) Viscous heat generation in slit flow. *AIChE J* 26:751–762